Molecular Therapy
Nucleic Acids
Original Article

A Novel Mechanism of Doxorubicin Resistance and Tumorigenesis Mediated by MicroRNA-501-5p-Suppressed BLID

Yun-chao Xu,[1,8] Xu Liu,[1,8] Min Li,[1] Yan Li,[4] Chun-yan Li,[5] Ying Lu,[6] Jaceline Sanches,[1] Lu Wang,[1] Yue Du,[1] Li-min Mao,[6] Si-bo Zuo,[1,7] Hui-ting Liu,[1,7] Jie Shen,[6] Bo Wang,[1] Li Hou,[1] Lian-hong Li,[1] Jian-wu Tang,[1] Jing-fang Ju,[3] Hong-wei Guan,[2] and Bo Song[1]

[1]Department of Pathology and Forensics, College of Basic Medical Sciences, Dalian Medical University, Dalian 116044, China; [2]Department of Pathology, The First Affiliated Hospital of Dalian Medical University, Dalian 116011, China; [3]Translational Research Laboratory, Department of Pathology, Stony Brook University, Stony Brook, NY 11794, USA; [4]Department of Anatomy, College of Basic Medical Sciences, Dalian Medical University, Dalian 116044, China; [5]Department of Gastroenterology, The First Affiliated Hospital of Dalian Medical University, Dalian 116011, China; [6]Teaching Laboratory of Morphology, College of Basic Medical Sciences, Dalian Medical University, Dalian 116044, China; [7]Department of Clinical Medicine, Grade 2015, Dalian Medical University, Dalian 116044, China

Doxorubicin is a widely used anthracycline-based anti-tumor agent for both solid and liquid tumors. Mounting evidence has demonstrated that microRNAs (miRNAs) are involved in chemoresistance and tumorigenesis. However, the roles of microRNA-501-5p (miR-501) in doxorubicin resistance and gastric cancer cell proliferation and invasion are still not fully understood. In this study, we identified that BLID (BH3-like motif-containing protein, cell death inducer) was directly regulated by miR-501 at the post-transcriptional level in multiple gastric cancer cell lines. Endogenous miR-501 was higher, whereas BLID was lower, in doxorubicin-resistant gastric cancer SGC7901/ADR cells compared with their parental SGC7901 cells. miR-501 suppressed gastric cancer cell apoptosis, induced resistance to doxorubicin, and enhanced cell proliferation, migration, and invasion. Subcutaneous injection of miR-501 lentivirus-infected SGC7901 cells resulted in rapid growth of xenograft tumors and resistance to doxorubicin treatment, unlike injection of negative miRNA lentivirus-infected SGC7901 cells. This is achieved at least partially by directly targeting BLID and subsequent inactivation of caspase-9 and caspase-3 and phosphorylation of Akt. Taken together, miR-501 induces doxorubicin resistance and enhances the tumorigenesis of gastric cancer cells by suppressing BLID. miR-501 might be a potential target for doxorubicin resistance and gastric cancer therapy.

INTRODUCTION

Gastric cancer is a digestive system malignancy and has the second-highest risk of cancer-related deaths worldwide, particularly in East Asia.[1,2] Chemotherapy has long been deemed to be a treatment option for locally advanced and metastatic gastric cancer in addition to radical surgery.[3] Doxorubicin (adriamycin [ADR]), an anthracycline-based anti-tumor agent, is effective for lymphoma and breast, lung, and gastric cancers when combined with other chemotherapeutic drugs, including fluorouracil and mitomycin. It was initially recommended as a gold standard therapy of advanced gastric cancer in 1980.[4–6] However, the 5-year survival rate of gastric cancer patients is still unsatisfactory because of resistance to frequent administration of ADR.[7]

MicroRNAs (miRNAs) are a class of small noncoding RNAs with 19∼25 nucleotides (∼22 nt) that act as post-transcriptional regulators binding to the 3′ UTR of target mRNA and, ultimately, alter mRNA translation or stability.[8] Over the past decade, miRNAs have been demonstrated to functionally participate in drug resistance in multiple tumor types.[9,10] miRNAs have also been reported to be involved in the mechanisms of doxorubicin resistance in gastric cancer.[11–13]

The gene encoding hsa-microRNA-501-5p (miR-501) is located on chromosome X. Several recent studies have demonstrated that miR-501 is upregulated in liver cancer,[14,15] gastric cancer,[16] lung adenocarcinoma,[17] and cervical cancer.[18] Moreover, high miR-501 is associated with advanced lung adenocarcinoma[17] and cervical cancer[18] and is an indicator of a poor prognosis in gastric cancer.[16] Thus, miR-501 may represent a novel oncogene. However, there is a lack of direct evidence of a link between miR-501 and doxorubicin resistance.

BLID (BH3-like motif-containing protein, cell death inducer), also known as breast cancer cell 2 (BRCC2), is a member of the Bcl-2

Received 16 January 2018; accepted 25 June 2018;
https://doi.org/10.1016/j.omtn.2018.06.011.

[8]These authors contributed equally to this work.

Correspondence: Bo Song, Department of Pathology and Forensics, College of Basic Medical Sciences, Dalian Medical University, Dalian 116044, China.
E-mail: songbo9177@163.com
Correspondence: Hong-wei Guan, Department of Pathology, The First Affiliated Hospital of Dalian Medical University, Dalian 116011, China.
E-mail: mudghw@aliyun.com

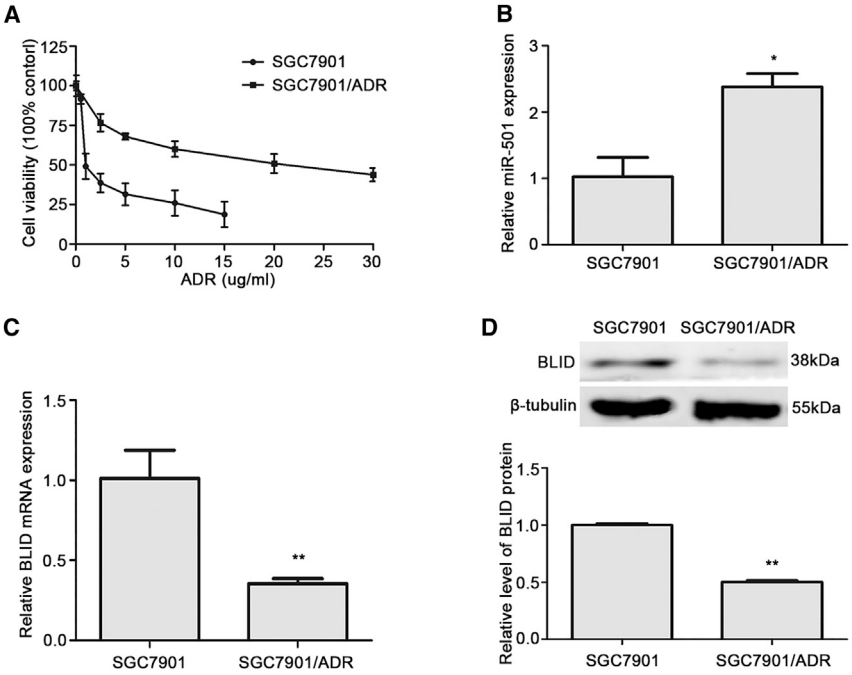

Figure 1. The Endogenous Level of miR-501 Is Higher and that of BLID Is Lower in SGC7901/ADR Cells Than in SGC7901 Cells

(A) The IC_{50} of doxorubicin in SGC7901 and SGC7901/ADR cells was detected by CCK8 assay. (B) The endogenous level of miR-501 in these two cell lines was detected by real-time qRT-PCR analysis. The expression level of miR-501 was normalized by the internal control RNU6B. (C) The endogenous level of BLID in these two cell lines was measured by real-time qRT-PCR, and GAPDH was the internal control. (D) Western blot analysis determined the endogenous expression of BLID protein, and β-tubulin was the internal control. All data are mean ± SD of three independent assays. *$p < 0.05$, **$p < 0.01$.

family. Broustas et al.[19,20] reported that BLID induces apoptosis either in a caspase-dependent manner through activating caspase-3 and caspase-9 or by interacting with Bcl-X_L. Another study found that BLID suppresses breast cancer cell growth and metastasis *in vitro* and *in vivo* by downregulating the Akt pathway.[21] BLID can be an independent predictor of prognosis and distant metastasis in breast cancer.[20,22] Apoptosis inhibition has been considered to be a critical mechanism of doxorubicin resistance.[23,24] Interestingly, the miRNA analysis software TargetScan (http://www.targetscan.org/) predicted that BLID is a potential target of miR-501. Therefore, we reasoned that miR-501 may enhance doxorubicin resistance in gastric cancer through suppressing apoptosis mediated by downregulation of BLID.

In this study, we revealed a novel mechanism of doxorubicin resistance mediated by miR-501 and investigated the functional significance of miR-501 in multiple gastric cancer cell lines, including SGC7901, SGC7901/ADR, and BGC823. We found that the endogenous level of miR-501 was higher in doxorubicin-resistant gastric cancer SGC7901/ADR cells compared with their parental SGC7901 cells, whereas that of BLID was lower in SGC7901/ADR cells. BLID was confirmed to be the direct target of miR-501 via luciferase reporter assay. Gain- and loss-of-function *in vitro* experiments showed that miR-501 suppressed gastric cancer cell apoptosis and induced resistance to doxorubicin. Moreover, miR-501 accelerated gastric cancer cell proliferation, migration, and invasion. Subcutaneous injection of nude mice with miR-501 lentivirus-infected SGC7901 cells resulted in rapid growth of tumors, unlike injection of control SGC7901 cells. Importantly, the volume of xenografts induced by miR-501 lentivirus-transduced SGC7901 cells was larger after being treated with doxorubicin compared with the control group. This is possibly achieved via downregulation of BLID and subsequent inactivation of caspase-9 and caspase-3 and phosphorylation of Akt. *In vivo* miR-501 inhibition showed the opposite effects compared with miR-501 overexpression. As a result, miR-501 induces doxorubicin resistance and enhances the tumorigenesis of gastric cancer cells by directly targeting BLID. miR-501 might be a potential target for doxorubicin resistance and gastric cancer therapy.

RESULTS

The Endogenous Expression Level of miR-501 Is Higher, whereas that of BLID Is Lower, in the Doxorubicin-Resistant Gastric Cancer Cell Line SGC7901/ADR Than in Its Parental Cell Line SGC7901

To investigate the role of miR-501 in doxorubicin resistance, we first compared the median growth inhibitory concentration (IC_{50}) of the gastric cancer cell line SGC7901/ADR and its parental cell line SGC7901. Our results showed that the IC_{50} of SGC7901/ADR cells was 10.65-fold higher than that of SGC7901 cells (Figure 1A). Then we quantified the endogenous levels of miR-501 and BLID mRNA in these paired gastric cancer cell lines by real-time quantitative RT-PCR (qRT-PCR). As shown in Figure 1B, the expression of miR-501 in SGC7901/ADR cells was significantly higher than that in the corresponding sensitive cells, whereas the expression level of BLID mRNA in SGC7901/ADR cells was dramatically lower (Figure 1C). Consistently, western blot analysis showed that BLID protein was reduced in SGC7901/ADR cells compared with SGC7901 cells (Figure 1D). These data indicate that miR-501 may induce doxorubicin resistance and that, possibly, there is a negative regulatory correlation between miR-501 and BLID. We then chose SGC7901 cells to perform knockin experiments, whereas SGC7901/ADR cells were used to perform knockdown treatments.

BLID Is a Direct Target of miR-501

Bioinformatics analysis of the miRNA database TargetScan (http://www.targetscan.org/) predicted that miR-501 has a potential binding

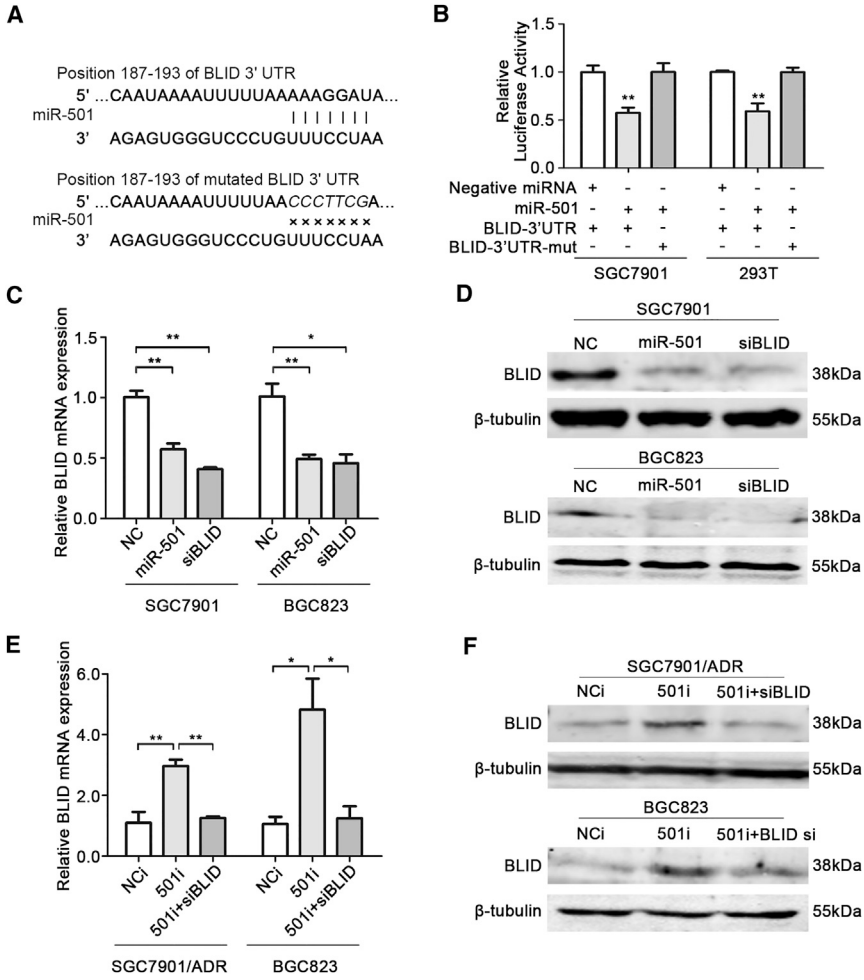

Figure 2. BLID Is Directly Targeted by miR-501

(A) An assumed miR-501 binding site existed in the 3′ UTR of BLID mRNA, and mutations were generated in the binding site. (B) The regulatory relationship between miR-501 and BLID was determined by luciferase assay. SGC7901 cells and 293T cells were co-transfected with a reporter luciferase plasmid (including wild-type or mutant BLID 3′ UTRs), a *Renilla* luciferase plasmid, and miRNA mimics. Firefly luciferase activity was normalized by the *Renilla* internal control. The value of relative luciferase activity for co-transfection of negative miRNA and the wild-type BLID 3′ UTR construct was set as 1, and the values for co-transfection of the miR-501 mimic and wild-type or mutant constructs were calculated as fold induction. (C and D) SGC7901 and BGC823 cells were transfected with the miR-501 mimic (miR-501) or siRNA against BLID (siBLID). Negative miRNA (NC) was the negative control, and siBLID was the positive control. The relative levels of BLID mRNA and protein were measured by real-time qRT-PCR (C) and western blot (D). GAPDH and β-tubulin were the internal controls, respectively. (E and F) SGC7901/ADR and BGC823 cells were transfected with the miR-501 inhibitor (501i). Scrambled miRNA inhibitor (NCi) and co-transfection of the miR-501 inhibitor and siBLID (501i + siBLID) were used as negative controls. BLID mRNA was examined by real-time qRT-PCR (E), and protein was examined by western blot (F). Data are indicated as mean ± SD. *$p < 0.05$, **$p < 0.01$.

site at positions 187 to 193 (AAAGGAT) in the 3′ UTR of BLID mRNA (Figure 2A). To confirm whether miR-501 directly alters the expression of BLID in gastric cancer cells, the wild-type 3′ UTR of BLID mRNA (BLID-3′ UTR) containing the miR-501 predicted binding site was inserted into the GV272 luciferase reporter vector. Our results showed that co-transfection of the miR-501 mimic and BLID-3′ UTR vector into SGC7901 and 293T cells evidently suppressed luciferase activity compared with co-transfection of negative miRNA and the BLID-3′ UTR vector (Figure 2B). As expected, the mutant 3′ UTR of BLID mRNA (BLID-3′ UTR-mut) failed to suppress luciferase activity upon transient overexpression of miR-501 (Figure 2B). Based on these results, we conclude that BLID is a direct target of miR-501 in gastric cancer cells.

To further disclose the regulatory correlation of miR-501 and BLID, SGC7901 cells were transfected with a miR-501 mimic (miR-501) or negative control miRNA (NC). BLID silenced by small interfering RNA (siRNA) specific for BLID (siBLID) was the positive control. The transfection efficiency of miR-501 was confirmed by real-time qRT-PCR analysis (Figure S1A). The expression of BLID at the mRNA and protein levels was then quantified by real-time qRT-PCR and western blot analyses. As shown in Figure 2C, left, ectopic expression of miR-501 led to a significant decrease in BLID mRNA compared with the NC group, whereas it was similar to the siBLID group. The western blot analysis showed that BLID protein was significantly reduced in miR-501 mimic-transfected and BLID knockdown SGC7901 cells (Figure 2D, top), indicating that miR-501 regulates BLID expression at the post-transcriptional level.

In addition, we used SGC7901/ADR cells to perform a loss-of-function analysis by knocking down endogenous miR-501. Scrambled miRNA inhibitor (NCi) and co-transfection of miR-501 inhibitor (501i) and siBLID (501i + siBLID) were used as negative controls. Real-time qRT-PCR and western blot analyses revealed that knockdown of miR-501 restored the expression of BLID mRNA and protein compared with the negative controls (Figures 2E, left, and 2G, top).

In addition to SGC7901 and SGC7901/ADR cells, we also confirmed the regulatory correlation of miR-501 and BLID in the gastric cancer cell line BGC823. After successful transfection of the miR-501 mimic (Figure S1B), we found that the expression of BLID at the mRNA and protein levels was significantly suppressed (Figures 2C, right, and 2D, bottom). Knockdown of miR-501 restored the expression of BLID mRNA and protein compared with the negative controls (Figures

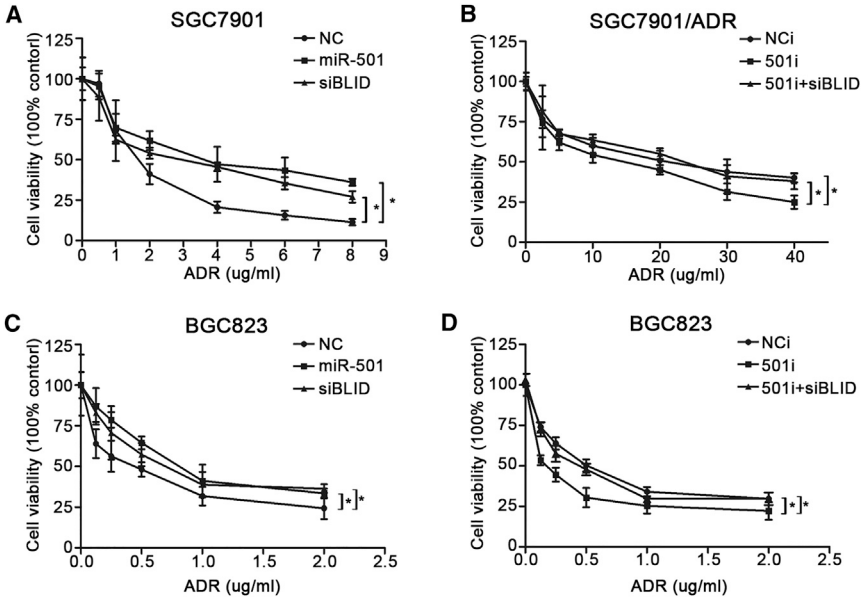

Figure 3. miR-501 Improves the Resistance to Doxorubicin in Gastric Cancer Cells

(A and C) After transfection with miR-501 and siBLID, SGC7901 (A) and BGC823 (C) cells were treated with different concentrations of doxorubicin for 48 hr. Cell viability was assessed by CCK8 assay. Negative miRNA (NC) was the negative control. The statistical significance indicates comparisons between miR-501 and NC and between siBLID and NC, respectively. (B and D) After transfection with 501i, SGC7901/ADR (B) and BGC823 (D) cells were treated with different concentrations of doxorubicin for 48 hr. Cell viability was assessed by CCK8 assay. Scrambled miRNA inhibitor (NCi) and co-transfection of miR-501 inhibitor and siBLID (501i + siBLID) were used as negative controls. The statistical significance indicates comparisons between 501i and NCi and between 501i and 501i + siBLID, respectively. Data represent the mean ± SD of three independent experiments. *$p < 0.05$.

2E, right, and 2G, bottom). These data firmly demonstrate that BLID is directly regulated by miR-501 at the post-transcriptional level.

miR-501 Induces Resistance to Doxorubicin in Gastric Cancer Cells by Targeting BLID

To determine the effects of miR-501 on chemoresistance, we used a series of different concentrations of doxorubicin to treat SGC7901 cells transfected with the miR-501, NC, or siBLID. The CCK8 assay revealed that miR-501 overexpression and BLID knockdown significantly enhanced the cell viability with doxorubicin treatment compared with NC (Figure 3A). On the contrary, 501i-transfected SGC7901/ADR cells were more sensitive to doxorubicin compared with the two negative controls (Figure 3B).

To further verify the roles of miR-501 in doxorubicin resistance in gastric cancer, the same process was performed in BGC823 cells. Overexpression of miR-501 induced doxorubicin resistance, and silenced BLID showed the same trend (Figure 3C). Conversely, downregulation of miR-501 promoted BGC823 cell sensitivity to doxorubicin (Figure 3D). Our findings suggest that miR-501 promotes resistance of gastric cancer cells to doxorubicin, possibly by downregulating BLID.

The miR-501/BLID Axis Enhances Resistance to Doxorubicin by Depressing Apoptosis via Caspase Pathway Inactivation

Anti-apoptosis has been considered a critical mechanism of doxorubicin resistance.[23,24] We tested the effects of miR-501 on apoptosis using an Annexin V-fluorescein isothiocyanate (FITC) and propidium iodide (PI) flow cytometry assay. A significant inhibition of the apoptotic rate (over 30%) was observed in the miR-501 group compared with the NC group in SGC7901 cells, whereas silenced BLID had a similar effect as miR-501 overexpression (Figure 4A). Activation of the caspase pathway has been reported to mediate the apoptosis caused by BLID.[19] We next analyzed the level of cleaved caspase-9 by western blot. As shown in Figure 4C, cleaved caspase-9 was inhibited in SGC7901 cells transiently transfected with the miR-501 mimic or BLID siRNA. Cleavage of procaspase-9 leads to the activation of caspase-3; here we also observed a low level of active caspase-3 (Figure 4C).

In contrast, SGC7901/ADR cells transfected with the 501i had a higher apoptotic rate than those transfected with the NCi (Figure 4E). Cleaved caspase-9 and caspase-3 expression was also increased by knockdown of miR-501 (Figure 4G). Similar results were obtained in BGC823 cells, as shown in Figures 4B, 4D, 4F, and 4H. These data demonstrate that the miR-501/BLID axis enhances doxorubicin resistance by depressing apoptosis via caspase pathway inactivation.

miR-501 Accelerates Gastric Cancer Cell Proliferation, Migration, and Invasion by Downregulating BLID and the Subsequent Phosphorylation of Akt

Some miRNAs acting as either oncogenes or tumor suppressors have been identified. To investigate the function of miR-501 in gastric cancer, we first performed a colony formation assay to determine the effects of miR-501 on cell proliferation in SGC7901 and BGC823 cells. As shown in Figure 5A and Figure S2A, miR-501 overexpression and BLID downregulation dramatically increased the colony formation efficiency compared with the negative control.

Subsequently, we assessed the influence of miR-501 on cell migration and invasion using transwell chamber assays. The transwell migratory assay (without Matrigel) showed that miR-501 overexpression significantly increased the numbers of SGC7901 and BGC823 cells passing

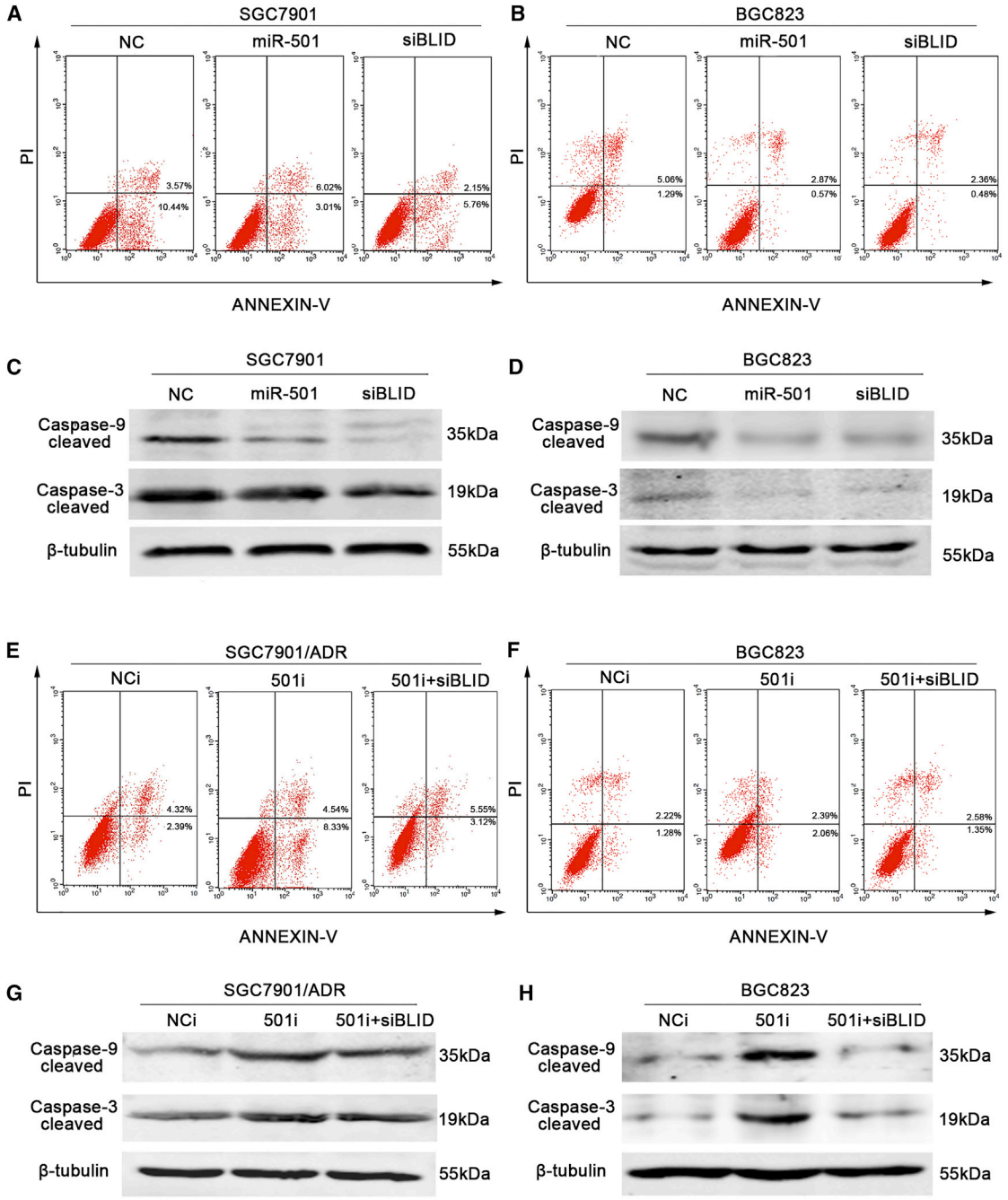

Figure 4. miR-501 Depresses Apoptosis via Caspase Pathway Inactivation

(A and B) SGC7901 (A) and BGC823 (B) cells were transfected with miR-501, NC, or siBLID, respectively. The apoptotic rate was examined using flow cytometry analysis. (C and D) Cleaved caspase-9 and caspase-3 were detected by western blot in the SGC7901 (C) and BGC823 (D) cells as grouped above. (E and F) SGC7901/ADR (E) and BGC823 (F) cells were transfected with 501i or NCi. The apoptotic rate was evaluated by flow cytometry. Co-transfection of 501i and siBLID (501i + siBLID) was also used as the negative control. (G and H) Cleaved caspase-9 and caspase-3 were detected by western blot in the SGC7901/ADR (G) and BGC823 (H) cells as grouped above. These experiments were performed three times, and the data are shown as mean ± SD. *$p < 0.05$, **$p < 0.01$.

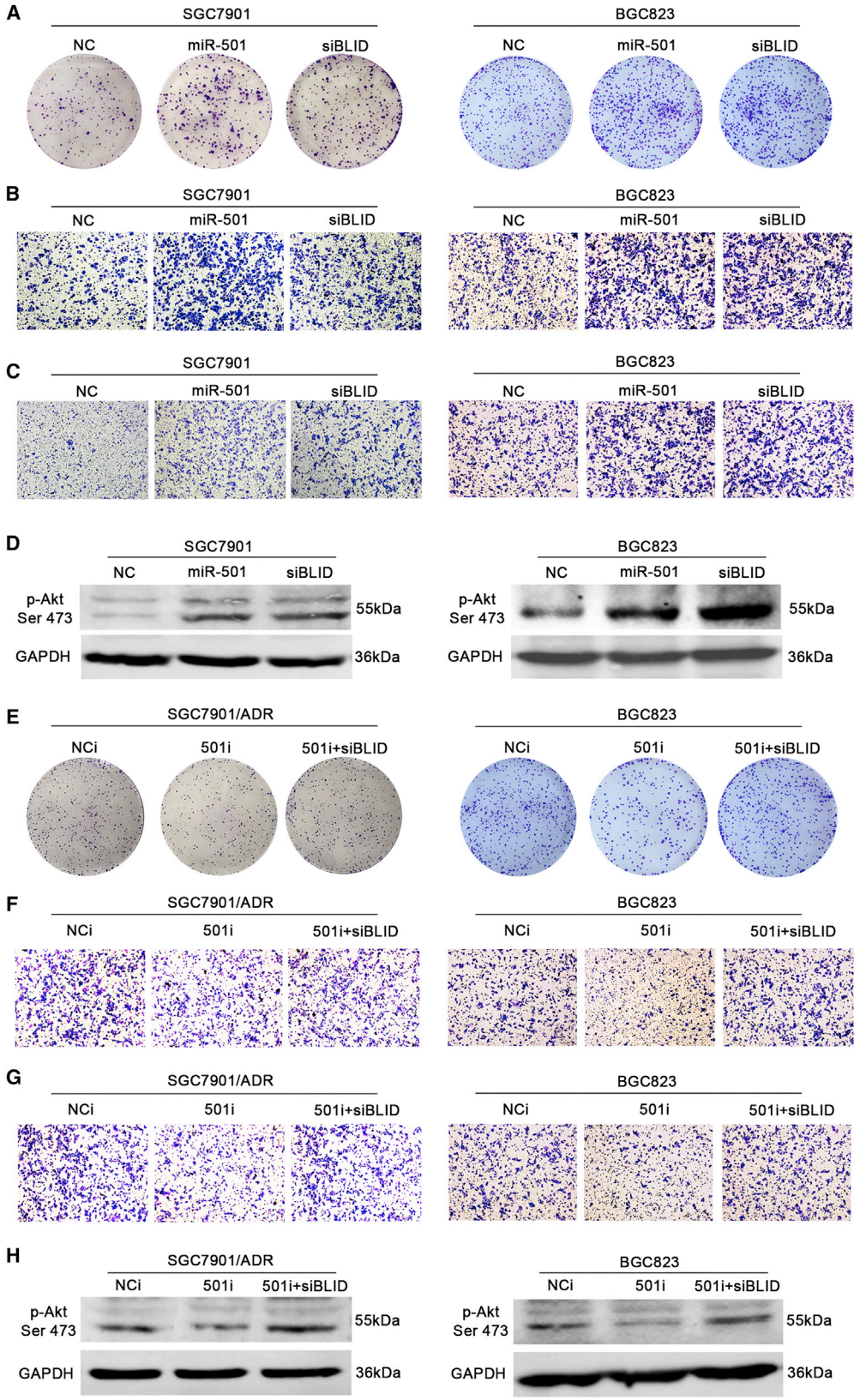

(legend on next page)

through the chamber compared with the negative control (Figures 5B and S2B). Equally, BLID knockdown promoted the migratory capacity of SGC7901 and BGC823 cells compared with the negative control (Figures 5B and S2B). The transwell invasion assay (with Matrigel) showed that the numbers of SGC7901 and BGC823 cells with miR-501 overexpression penetrating through the membrane were remarkably higher than those of the negative control group, whereas silenced BLID had a similar trend with miR-501 overexpression (Figures 5C and S2C). Briefly, miR-501 increases the capacity for proliferation, migration, and invasion of gastric cancer cells, possibly by downregulating BLID.

The phosphatidylinositol 3-kinase (PI3K)/Akt pathway has essential roles in the proliferation, migration, and invasion of numerous cancer types, including gastric cancer.[25] Additionally, Li et al.[21] reported that BLID suppresses breast cancer cell growth and metastasis by downregulating the Akt pathway. Thus, we measured the phosphorylation profile of Akt at Ser 473. As shown in Figure 5D, upregulation of miR-501 and knockdown of BLID dramatically activated the phosphorylation of Akt at Ser 473 compared with the negative miRNA-transfected counterpart in SGC7901 and BGC823 cells.

Conversely, knockdown of miR-501 inhibited the proliferation, migration, and invasion potential in SGC7901/ADR and BGC823 cells (Figures 5E–5G and S2D–S2F). Consistently, the phosphorylation of Akt at Ser 473 was depressed compared with the NCi and the 501i + siBLID counterparts (Figure 5H). Taken together, our findings imply that miR-501 increases gastric cancer cell proliferation, migration, and invasion by downregulating BLID and the subsequent activation of the Akt pathway.

miR-501 Induces Doxorubicin Resistance and Enhances the Carcinogenesis of Gastric Cancer *In Vivo*

Given the observed effects of miR-501 on doxorubicin resistance and gastric cancer cell behavior *in vitro*, we subsequently investigated whether miR-501 can induce doxorubicin resistance and enhance carcinogenesis *in vivo*. We infected SGC7901 cells with lentiviral vectors of miR-501 (Len-501), negative control (Len-NC), or short hairpin RNA (shRNA) against BLID (shBLID) and screened the infected cells using puromycin. We observed that more than 90% of cells had green fluorescence under the fluorescence microscope (Figure 6A). Moreover, the expression of miR-501 and BLID was verified using real-time qRT-PCR and western blot analyses (Figures S3A–S3C). We then injected these cells subcutaneously into nude mice and monitored subcutaneous tumor growth. We found that the tumors in the Len-501 group grew faster than those in the Len-NC group and that BLID silenced by shRNA appeared as a similar trend compared to the Len-501 group (Figure 6B). When the size of xenograft tumors of each group reached 100 mm^3, the mice were administered ADR through the tail vein three times per week. After 2 weeks of ADR treatment, the mice were sacrificed. We found that both the Len-501 group and the shBLID group had significantly larger tumor volumes than the Len-NC group (Figures 6C and 6D). These results indicate that miR-501 overexpression may induce doxorubicin resistance and promote the growth of gastric cancer cells *in vivo*.

We then detected the expression of miR-501 and its target BLID at both the mRNA and protein levels in mouse xenograft tumor tissues using real-time qRT-PCR and western blot analyses. Representative results are shown in Figures 6E–6G. Briefly, miR-501 was significantly upregulated by approximately 17-fold in the Len-501 group compared with the Len-NC group, whereas BLID was markedly downregulated at both the mRNA and protein levels in the Len-501 group and shBLID group compared with the Len-NC group.

We then investigated the underlying mechanism of miR-501 enhancement on drug resistance and carcinogenesis *in vivo*. The protein levels of cleaved caspase-9 and caspase-3 were decreased, and the phosphorylation of Akt was increased dramatically, in Len-501-injected xenograft tumor tissues compared with Len-NC, as determined by western blot analysis (Figure 6H).

To further clarify the roles of miR-501 on doxorubicin resistance and tumorigenesis *in vivo*, knockdown of miR-501 in SGC7901/ADR cells was performed. We infected SGC7901/ADR cells with lentiviral vectors of the 501i (Len-501i) and NCi (Len-NCi), respectively. Co-infection of lentiviral vectors of 501i and shRNA against BLID (Len-501i + shBLID) was the negative control as well. As shown in Figure S4A, most SGC7901/ADR cells presented green fluorescence. miR-501 expression was dramatically reduced, and BLID expression at both the mRNA and protein levels was increased, in the Len-501i group compared with the negative control groups (Figures S4B–S4D), indicating successful infection of 501i lentiviral vectors. We then injected these cells subcutaneously into nude mice and found that subcutaneous tumor growth was suppressed in the Len-501i group compared with the Len-NCi and the Len-501i + shBLID groups (Figure S4E). After ADR treatment, the Len-501i group had significantly smaller tumor volumes than the Len-NCi group and the Len-501i + shBLID group (Figure S4F). miR-501 expression was reduced, and BLID mRNA expression was increased, in mouse xenograft tumor tissues (Figures S4G and S4H), and the protein expression of BLID

Figure 5. miR-501 Accelerates Gastric Cancer Cell Proliferation, Migration, and Invasion via the Phosphorylation of Akt

(A) SGC7901 and BGC823 cells were transfected with the miRNA mimics or siRNA described as above. A colony formation assay was performed to show the effect of miR-501 on cell growth. (B) Cell migratory potential was determined by transwell migration assay without Matrigel. (C) Cell invasive potential was determined by transwell invasion assay with Matrigel. (D) The phosphorylation of Akt Ser 473 (p-Akt Ser 473) was detected by western blot. (E) Endogenous miR-501 was knocked down by the inhibitor in SGC7901/ADR and BGC823 cells. The cell proliferative potential was detected by colony formation assay. Transwell assays with or without Matrigel were performed to determine the potential of migration (F) and invasion (G) in miR-501 knockdown SGC7901 cells and BGC823 cells, respectively. (H) The protein expression of p-Akt Ser 473 was determined using western blot. All experiments were repeated three times, and the data are indicated as mean ± SD. *$p < 0.05$, **$p < 0.01$.

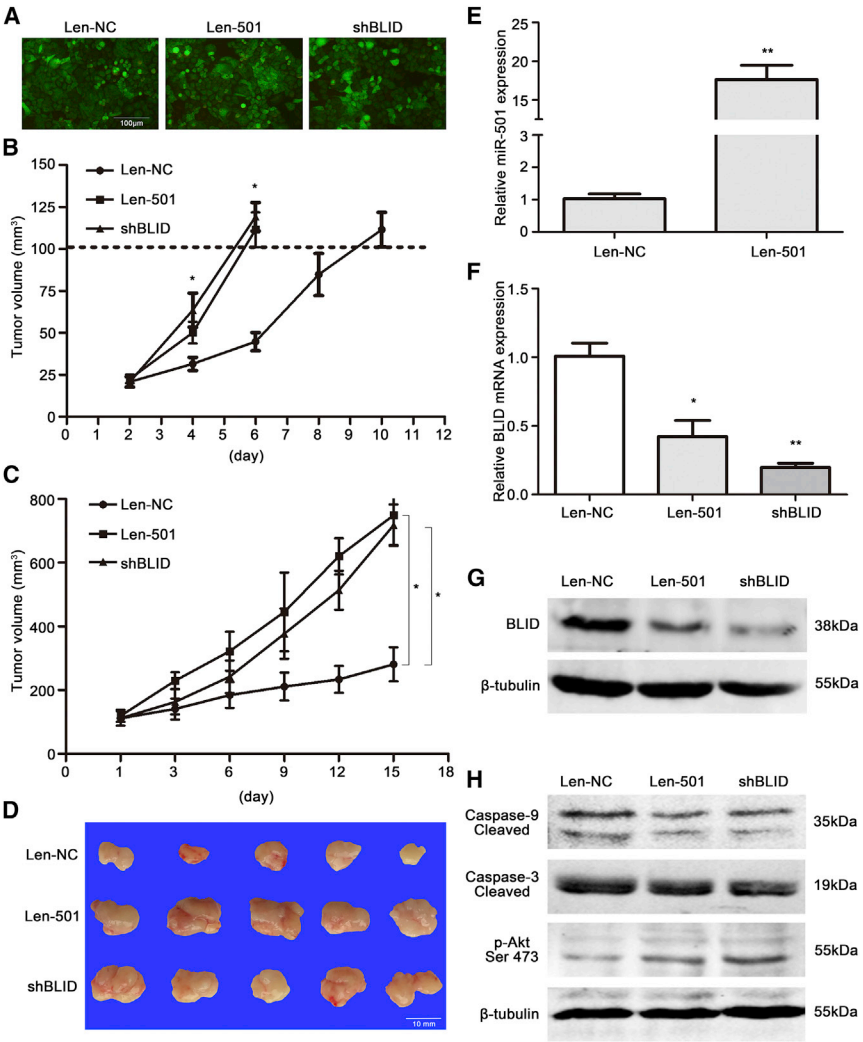

Figure 6. miR-501 Induces Doxorubicin Resistance and Enhances the Growth of Gastric Cancer Cells *In Vivo*

(A) SGC7901 cells were infected with lentiviral vectors of miR-501 (Len-501), negative miRNA (Len-NC), or shRNA against BLID (shBLID), and more than 90% of cells had green fluorescence under the fluorescence microscope. Representative microscopic pictures were taken. (B) The size of subcutaneous tumors in nude mice was measured every 2 days after injection until reaching 100 mm^3. A growth rate curve is shown. (C and D) The mice were administered ADR through the tail vein three times per week for 2 weeks. The tumor volumes were measured and recorded at all time points (C), and the xenografts were shown in (D). (E) The expression of miR-501 in tumor xenografts was quantified by real-time qRT-PCR. (F) The expression of BLID mRNA in mouse xenograft tumor tissues was detected using real-time qRT-PCR. (G and H) The protein expression of BLID (G), cleaved caspase-9/3, and p-Akt Ser 473 (H) in the xenograft tumor tissues was analyzed by western blot. Data are indicated as mean ± SD. *$p < 0.05$, **$p < 0.01$.

and cleaved caspase-9 and caspase-3 was increased, and the phosphorylation of Akt was decreased (Figure S4I). Taken together, these results suggest that miR-501 promotes doxorubicin resistance and growth of gastric cancer cells *in vivo*, probably by downregulating the expression of BLID and subsequent inactivation of the caspase pathway and phosphorylation of Akt.

miR-501 Is Upregulated in Human Gastric Cancer Tissues, and High miR-501 Expression Predicts a Poor Prognosis

By analysis of The Cancer Genome Atlas (TCGA) stomach adenocarcinoma miRNA sequencing datasets, we found that miR-501 expression was dramatically upregulated in human gastric cancer tissues (n = 316) compared with normal gastric tissues (n = 50, $p < 0.0001$; Figure S5A). Furthermore, patients with high miR-501 expression (n = 107) had a significant poor overall survival rate compared with those with low miR-501 expression (n = 107, $p < 0.0001$; Figure S5B). These results indicate that miR-501 overexpression is probably related to the development of gastric cancer and represents a poor prognostic factor.

Based on our results above, a model was proposed for the potential roles of miR-501 in gastric cancer (Figure 7). miR-501 triggers doxorubicin resistance by inhibiting apoptosis mediated by the suppression of BLID and subsequent inactivation of caspase-9 and caspase-3. miR-501 also enhances gastric cancer growth and progression through inhibition of BLID and phosphorylation of Akt.

DISCUSSION

Chemotherapy, one of the principal approaches for gastric cancer treatment, plays a crucial role in controlling tumor progression.[1] However, most patients sooner or later become resistant to anticancer agents, particularly doxorubicin, after repeated treatment.[26] Although research has increasingly explored the mechanisms of chemoresistance, such as increased drug efflux, mutation of target genes, inactivation of detoxification enzymes, dysfunction of proapoptotic proteins, or enhancement of DNA repair activity,[27,28] the mechanisms involved in cancer cell chemoresistance are still not fully understood. In recent years, mounting evidence has shown that miRNAs are critical regulators of chemoresistance in a variety of cancers, including gastric cancer.[11,29] Our group has previously investigated the effects and mechanisms of miR-140 and miR-215 on resistance to methotrexate (MTX), 5-fluorouracil (5-FU), and Tomudex (TDX).[30,31] In the current study, we present original evidence that miR-501 induces doxorubicin resistance and enhances the tumorigenesis of gastric cancer cell by targeting BLID.

BLID is a novel tumor suppressor gene that was initially investigated in breast cancer.[19] A recent study reported that miR-575 targets BLID

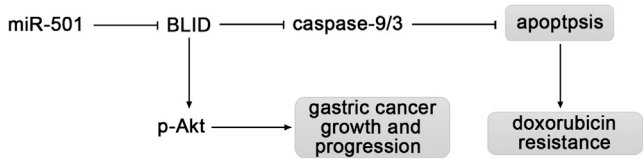

Figure 7. Proposed Model of miR-501 Function in Gastric Cancer
miR-501 downregulates BLID, a cell death inducer, and subsequently inactivates caspase-9/3, resulting in inhibition of apoptosis, thereby inducing doxorubicin resistance. Downregulation of BLID by miR-501 promotes gastric cancer growth and progression through enhanced phosphorylation of Akt.

in non-small-cell lung cancer (NSCLC) cells and that BLID is downregulated in NSCLC tissues compared with adjacent normal lung tissues.[32] We experimentally confirmed, for the first time to our best knowledge, that BLID was directly targeted by miR-501 in gastric cancer cells and that miR-501 reduced the expression of BLID at both the mRNA and protein levels. Importantly, our *in vitro* and *in vivo* results from gain- and loss-of-function experiments indicated that miR-501 induced resistance to doxorubicin in gastric cancer. Although resistance to doxorubicin is a phenomenon involving multiple factors, alterations in apoptosis-related genes play an important role.[23,24] Broustas et al.[19] reported that BLID functions as a pro-apoptotic molecule in a caspase-dependent manner. To explore the mechanism of miR-501 in doxorubicin resistance, we examined the apoptotic rate using flow cytometry. We found that miR-501 inhibited gastric cell apoptosis under the stress situation of doxorubicin treatment. The western blot analysis showed that cleaved caspase-9 and caspase-3 were decreased along with the downregulation of BLID. Our data suggest that miR-501 directly targets BLID to inhibit apoptosis and, hence, promotes chemoresistance to doxorubicin. In addition to the caspase pathway, BLID can induce apoptosis by interacting with Bcl-X_L.[20] However, this remains to be determined and added to the explanation of miR-501-induced doxorubicin resistance in our future study.

In addition to inducing doxorubicin resistance, our present study showed that miR-501 enhanced the proliferation, migration, and invasion of gastric cancer cells. Subcutaneous injection of miR-501 lentivirus-infected SGC7901 cells into nude mice resulted in faster growing tumors than injection with control SGC7901 cells. miR-501 knockdown SGC7901/ADR cells grew at a slow rate in nude mice. Based on the notion that overexpression of BLID significantly inhibits the phosphorylation of Akt to suppress breast cancer cell growth and metastasis,[20] we evaluated the phosphorylation of Akt Ser 473. Our results indicated that phosphorylation of Akt Ser 473 was upregulated, whereas BLID was downregulated, by miR-501 in gastric cancer. The subsequently increased MMP-2 and MMP-9 may contribute to the enhanced metastatic ability.[21] Therefore, miR-501 enhances the tumorigenesis of gastric cancer cells, possibly by downregulating BLID and activating the Akt pathway. Consistent with our findings, a recent study of gastric cancer revealed that miR-501 activates wnt/β-catenin signaling to enhance the cancer stem cell-like phenotype by directly targeting DKK1, NKD1, and GSK3β *in vitro*.[16] Fan et al.[16] found that miR-501 expression is markedly increased in gastric cancer samples compared with non-cancerous gastric tissues and that patients with a high miR-501 level have poor overall survival. We also found that miR-501 was highly expressed in gastric cancer samples and that miR-501 overexpression was related to a poor prognosis of gastric cancer patients based on TCGA data analysis. However, there are no available data of BLID expression in gastric cancer. Our group is collecting clinical gastric cancer samples and plans to evaluate the expression and clinical significance of miR-501 and its direct target, BLID, in gastric cancer. In addition to the targets above, Huang et al.[14] found that CYLD (cylindromatosis) is a direct target gene of miR-501 and that miR-501 promotes the proliferation of hepatocellular carcinoma (HCC) cells via decreased CYLD expression and increased expression of cyclin D1 and c-*myc in vitro*. Our group also found that miR-501 enhances cervical cancer cell proliferation, migration, and invasion, possibly by downregulating CYLD and subsequently activating nuclear factor κB (NF-κB) p65. miR-501 overexpression and CYLD downregulation are associated with the development and progression of cervical cancer.[18] Another study reported that miR-501 is upregulated in clinical HCC specimens and that miR-501 may improve the replication of hepatitis B virus (HBV) by targeting HBXIP.[15] Very recently, miR-501 was found to be overexpressed in lung adenocarcinoma from the Xuanwei area of China, and higher miR-501 expression is associated with the tumor-node-metastasis (TNM) stages.[17] These data indicate that miR-501 may function as an oncogene in gastric, liver, lung, and cervical cancer and that it plays a vital role in tumorigenesis and progression.

In addition to CYLD, DKK1, NKD1, GSK3β, HBXIP, and BLID, discussed above, we also searched for some tumor suppressors as potential targets of miR-501 using TargetScan.

Cyclin-dependent kinase inhibitor 2B (CDKN2B), also known as p15, inhibits cyclin-dependent kinase 4 (CDK4) or CDK6 to control G1 cell cycle progression.[33] CDKN2B gene loss has been found in gastric cancer.[34–36] Li et al.[37] found that the expression of CDKN2B is reduced in colorectal cancer (CRC) tissue and that miR-18b enhances the tumorigenesis of CRC by targeting CDKN2B. GADD45G (originally termed Gadd45, MyD118, and CR6/GRP17) is a member of the growth arrest DNA damage-inducible gene (GADD45) family except for GADD45A and GADD45B.[38] Guo et al.[39] reported that the GADD45G gene acts as a tumor suppressor but is frequently inactivated epigenetically in gastric cardia adenocarcinoma patients. Zhang et al.[40] also found that GADD45G methylation is higher in gastric, colorectal, and pancreatic cancer than in normal tissue. Low-density lipoprotein receptor-related protein 1B (LRP1B) was reported to be highly methylated in gastric cancer samples, and ectopic overexpression of LRP1B4 suppresses gastric cancer cell growth, colony formation, and tumor formation in nude mice, indicating that LRP1B is a functional tumor suppressor in gastric cancer.[41] Wu et al.[42] found that glutamate receptor, ionotropic, kainate 2 (GRIK2) functions as a tumor suppressor in gastric cancer as being methylated. GRIK2-expressing gastric cancer cells show decreased colony formation and cell

migration abilities. The potential targets of miR-501 also include early B cell factor 3 (EBF3) and opioid binding protein/cell adhesion molecule-like (OPCML).[43,44] miR-501 might play a role in gastric cancer by targeting these genes; however, this still needs to be confirmed.

Currently our comprehension of miR-501 function is still limited, and, in particular, little is known about its roles in chemoresistance to doxorubicin. We are just beginning to understand the effects and significance of miR-501 in gastric cancer. Additional genes and pathways regulated by miR-501 may contribute to doxorubicin resistance and gastric cancer growth. Our future studies will focus on further disclosing the underlying molecular regulatory mechanisms of miR-501 function and investigating the expression of BLID and its clinicopathologic significance in gastric cancer.

Conclusions

In conclusion, our findings demonstrate that miR-501 induces chemoresistance to doxorubicin and enhances tumorigenesis in gastric cancer, at least partially by directly targeting BLID and the subsequent inactivation of the caspase pathway and phosphorylation of Akt. miR-501 perhaps functions as an oncogene, and therapy based on miR-501 may improve the anticancer effect in gastric cancer.

MATERIALS AND METHODS

Cell Culture and Reagents

The human doxorubicin-resistant gastric cancer cell line SGC7901/ADR and its parental cell line SGC7901 were kind gifts from the Department of Digestive Diseases of Xijing Hospital, Fourth Military Medical University (Xi'an, China). The human gastric cancer cell line BGC823 was a kind gift from Prof. Yan Li at the Department of Anatomy of Dalian Medical University (Dalian, China). Cells were cultured in RPMI 1640 medium (Gibco, Grand Island, NY) supplemented with 10% fetal bovine serum (FBS) and antibiotics in a 37°C incubator in a humidified atmosphere with 5% CO_2. Doxorubicin (0.5 μg/mL) (Haizheng, Zhejiang, China) was sustained in the culture medium to maintain drug resistance for SGC7901/ADR cells. SGC7901/ADR cells were cultured in drug-free medium for at least 7 days before initiating the experiments.

Cell Transfection

For gain-of-function experiments, SGC7901 and BGC823 cells (3×10^5 per well) were plated in 6-well plates and then transfected with 100 nM of either miR-501 mimic, negative miRNA (Invitrogen, Carlsbad, CA), or siRNA specific for BLID (Invitrogen, Carlsbad, CA) after 24 hr with Lipofectamine 2000 (Invitrogen, Carlsbad, CA) according to the manufacturer's protocol. The transfected cells were prepared for RNA and protein extraction 24 hr and 48 hr after transfection, respectively.

To knock down endogenous miR-501, SGC7901/ADR and BGC823 cells were plated in 6-well plates at 3×10^5 cells/well and then transfected with 100 nM of either miR-501 inhibitor or negative miRNA inhibitor (Invitrogen, Carlsbad, CA) with Lipofectamine 2000. Co-transfection with 50 nM of miR-501 inhibitor and 50 nM of siRNA specific for BLID was also used as a negative control. The transfected cells were harvested for RNA and protein extraction 24 hr and 72 hr after transfection, respectively.

RNA Extraction and Real-Time qRT-PCR Analysis

Total RNA, including miRNA, was extracted from SGC7901, SGC7901/ADR, and BGC823 cells with or without transfection using TRIzol reagent (Invitrogen, Carlsbad, CA). The frozen xenograft tumor tissues were ground using a prechilled pestle in a mortar at 4°C and processed using TRIzol reagent.

The cDNA of miRNA was synthesized using the TaqMan microRNA Reverse Transcription Kit (Life Technologies, Gaithersburg, MD). Real-time qRT-PCR analysis was performed on an Agilent MX3000P instrument (Agilent Technologies, Santa Clara, CA). The primers for miR-501 and the endogenous control RNU6B were purchased from Ambion (Austin, TX). The expression value of miR-501 was normalized to RNU6B and was calculated using the $2^{(-\Delta\Delta CT)}$ method.

For real-time qRT-PCR analysis of mRNA expression, cDNA was synthesized using the PrimeScript RT Reagent Kit with gDNA Eraser (TaKaRa, Dalian, China). The qRT-PCR amplification for BLID mRNA was performed with SYBR Premix Ex TaqII (TaKaRa, Dalian, China) according to the manufacturer's instructions and was calculated using the $2^{(-\Delta\Delta CT)}$ method after normalizing to GAPDH. All qRT-PCR experiments were done in triplicate. Primers are listed in Table S1.

Western Blot Analysis

Parental and transfected cells were lysed with 1× radioimmunoprecipitation assay (RIPA) buffer (Sigma-Aldrich, St. Louis, MO). The frozen mouse tumor tissues were crushed with a prechilled pestle in a mortar. Then extraction and solubilization were performed. The concentration of protein was measured by the Bradford method with BSA (Sigma-Aldrich, St. Louis, MO) as the standard. Equal amounts of protein extract (40 μg) were denatured with 10%–15% SDS-PAGE, transferred to polyvinylidene fluoride (PVDF) membranes (Millipore, Billerica, MA).The membranes were blocked with 5% non-fat milk in TBS Tween (TBST) (0.1 M, pH 7.4) and incubated with antibodies against BLID (1:200 diluted; Abcam, Cambridge, MA), cleaved caspase-9 and caspase-3 (1:500 diluted; Abcam, Cambridge, MA), and p-Akt Ser 473 (1:500 diluted; Abgent, San Diego, CA) at 4°C overnight. β-Tubulin (1:500 diluted; Abgent, San Diego, CA) served as a control for protein loading. Membranes were incubated with secondary antibodies, horseradish peroxidase (HRP)-conjugated rabbit or mouse anti-immunoglobulin G (IgG) (LI-COR Biosciences, Lincoln, NE), diluted at 1:16,000 in TBST, for 1 hr at room temperature. Protein bands were revealed using the Odyssey infrared imaging system (LI-COR Biosciences, Lincoln, NE).

Luciferase Assay

Double-stranded oligonucleotides of the BLID 3′ UTR (wild-type or mutant) were synthesized and inserted into the XbaI site of the

GV272 vector (GeneChem, Shanghai, China). The sequences of these synthesized wild-type and mutant 3′ UTRs of BLID mRNA are listed in Table S2.

SGC7901 cells were plated in triplicate in 24-well plates and cultured for 24 hr. Cells in each well were co-transfected with 100 nM of miR-501 mimic or negative miRNA and 200 ng of GV272 constructs containing wild-type or mutant 3′ UTR of BLID mRNA using Lipofectamine 2000, respectively. 20 ng of pRL-TK *Renilla* plasmid (Promega, Madison, WI) was added as the normalization. All cells were harvested 48 hr after transfection, and luciferase activity was measured using the Dual-Luciferase Reporter Assay System (Promega, Madison, WI). Firefly luciferase activity was normalized to the *Renilla* internal control for each condition and then compared with the negative miRNA-transfected wells. 293T cells were treated with the same method as described above to further verify the regulatory relationship between miR-501 and BLID.

Doxorubicin Treatment

Cells (1×10^4) were re-seeded in 96-well plates 24 hr after transfection. Twenty-four hours later, doxorubicin (0.5–40 μg/ml) in 100 μL medium was added and incubated for 72 hr. Then 10 μL of CCK8 solution (Sigma-Aldrich, St. Louis, MO) was added to each well. After 2 hr incubation at 37°C in 5% CO_2, the plates were read under 450-nm wavelength with a microplate reader (Thermo Scientific, Waltham, MA). Each experiment was performed in triplicate and repeated three times. The IC_{50} was calculated through growth curves.

Apoptosis Assay

To determine the level of cellular apoptosis, flow cytometry analysis was performed using the FITC Annexin V Apoptosis Detection Kit (BD Biosciences, Franklin Lakes, NJ). After treatment with doxorubicin for 48 hr, cells were washed twice with prechilled PBS, and then 5×10^5 cells were resuspended in 500 μL 1× binding buffer and mixed with 5 μL FITC Annexin V and 5 μL PI at room temperature (25°C) while avoiding light for 30 min. The stained cells were then counted using a fluorescence-activated cell sorting (FACS) flow cytometer (BD Biosciences, San Jose, CA).

Colony Formation Assay

Twenty-four hours after transfection, the cells were harvested and re-seeded in 6-well plates at 3×10^2 cells per well. The culture medium was replaced every 2 days during colony growth. 14 days after reseeding, the colonies were stained with 0.1% crystal violet for 30 min. The colonies were counted under an inverted phase contrast microscope (Olympus IX71; Olympus, Tokyo, Japan).

Transwell Migration and Invasion Assays

A transwell invasion assay was used to demonstrate the invasive ability of cells. Briefly, 60 μL of 1:5 diluted Matrigel (BD Biosciences, Franklin Lakes, NJ) was applied to the bottom of 24-well transwell chambers (Corning Life Sciences, New York, NY) and incubated at 37°C for 1 hr. After 24 hr of starving, 200 μL of suspension containing 2×10^5 cells were seeded into the upper chambers, whereas the lower chambers were placed into medium supplemented with 10% FBS (600 μL). After incubation at 37°C for 24 hr, cells on the upper side of the chambers were wiped gently with a cotton swab. The inserts were then fixed by 4% methanol for 15 min and stained with 0.1% crystal violet for 20 min. The average migratory cells were counted by randomly choosing five fields under the microscope. The experiments were repeated three times.

For the transwell migration assay, the remaining protocol was the same as the transwell invasion assay except for the pre-coating of the Matrigel in the inserts.

Lentivirus Infection

Lentiviral vectors of miR-501, lentiviral vectors of the 501i, the negative control, and shRNA against BLID were purchased from GeneChem (Shanghai, China). SGC7901 or SGC7901/ADR cells (1×10^5) were plated in 6-well plates and cultured until reaching about 50% confluence. A concentration of 10 μL of lentiviral vectors was added to infect the cells for 3 days. For the co-infection assay, 5 μL of 501i lentiviral vector and 5 μL of shRNA against the BLID lentiviral vector were added to co-infect SGC7901/ADR cells. Then 1 μM of puromycin (Sigma-Aldrich, St. Louis, MO) was used to screen lentivirus-infected cells. Cells expressing GFP were observed under fluorescence microscopy (Olympus IX73; Olympus, Tokyo, Japan). The expression of miR-501 and BLID in the infected cells was confirmed by western blot and qRT-PCR, respectively.

Mouse Xenograft Tumor Model

Thirty 6-week-old female BALB/c nude mice were purchased from the Experimental Animal Center of Dalian Medical University. For knockin experiments, mice were randomly divided into three groups. Group 1 was injected with lentivirus control-infected cells, group 2 was injected with lentivirus miR-501-infected cells, and group 3 was injected with shRNA against BLID-infected cells. In total, 1×10^6 infected cells in 100 μL PBS and Matrigel (BD Biosciences, Franklin Lakes, NJ) were subcutaneously injected into nude mice. The growth of subcutaneous tumors was monitored, and the subcutaneous tumor volume was calculated as follows: (greatest diameter) × (shortest diameter)^2 × 0.5. When the volume of xenografts reached approximately 100 mm^3, the mice were administered ADR (50 mg/kg) through the tail vein three times a week for 2 weeks. For knockdown experiments, mice were randomly divided into three groups. Group 1 was injected with lentivirus NCi control-infected cells, group 2 was injected with lentivirus 501i-infected cells, and group 3 was injected with lentivirus 501i and shRNA against BLID co-infected cells. When the volume of xenografts reached approximately 50 mm^3, the mice were administered ADR (50 mg/kg) through the tail vein three times a week for 2 weeks. The remaining procedures were the same as for the knockin experiments. The mice were sacrificed, and the subcutaneous tumors were excised and frozen in liquid nitrogen until processing for RNA and protein isolation. Animal care was conducted according to the guidelines. All studies involving mice were approved by the Animal Care and Use Committee of Dalian Medical University.

TCGA Dataset Analysis

The preprocessed level 3 RNA sequencing (RNA-seq) data and corresponding clinical information of gastric cancer patients were collected from the TCGA database (http://cancergenome.nih.gov/). In total, 366 samples (50 normal gastric tissues and 316 gastric cancer tissues) from the TCGA were included in the analysis.

Statistical Analysis

Statistical analysis was done using the SPSS software (version 11.0; IBM, Armonk, NY). The results were expressed as the mean ± SD. Statistical differences were determined using a two-tailed Student's t test between two groups. For comparison of more than two groups, one-way ANOVA followed by a Bonferroni-Dunn test was performed. For analysis of the TCGA dataset, Welch's t test was performed to test whether miR-501 expression is different between normal tissues and gastric cancer tissues. The first 33% of miR-501 expression in gastric cancer patients were placed in the high expression group (n = 107), and the last 33% were placed in the low expression group (n = 107). Survival curves were obtained using the Kaplan-Meier method and a log rank test. $p < 0.05$ was considered statistically significant.

SUPPLEMENTAL INFORMATION

Supplemental Information includes five figures and two tables and can be found with this article online at https://doi.org/10.1016/j.omtn.2018.06.011.

AUTHOR CONTRIBUTIONS

Conceptualization, B.S., H.G., and J.J.; Data Curation, Y.X., X.L., M.L., C.L., and Y. Lu; Formal Analysis, Y.X., X.L., M.L., C.L., Y. Li, J. Sanches, L.W., Y.D., L.M., S.Z., H.L., and L.H.; Investigation, Y.X., X.L., M.L., C.L., and Y. Lu; Methodology, Y.X., X.L., and M.L.; Project Administration, B.W.; Resources, Y.X., J. Shen, and B.W.; Supervision, B.S., H.G., and J.J.; Validation, Y.X. and X.L.; Visualization, Y.X., X.L., and M.L.; Writing – Original Draft, Y.X. and B.S.; Writing – Review & Editing, Y.X., L.L., J.T., B.S., and J.J.

CONFLICTS OF INTEREST

The authors declare that they have no competing interests.

ACKNOWLEDGMENTS

This work was supported by grants from the National Natural Science Foundation of China (81172052 to B.S.), the Natural Science Foundation of Liaoning Province (201602235 to B.S.), the "Yingcai" Program of Dalian Medical University (to B.S.), the Liaoning Provincial Program for Top Discipline of Basic Medical Sciences (to B.S.), and the Liaoning Province Innovative Training Project of College Students (2017101610100034 to S.Z. and H.L.).

REFERENCES

1. Siegel, R.L., Miller, K.D., and Jemal, A. (2018). Cancer statistics, 2018. CA Cancer J. Clin. *68*, 7–30.
2. Torre, L.A., Bray, F., Siegel, R.L., Ferlay, J., Lortet-Tieulent, J., and Jemal, A. (2015). Global cancer statistics, 2012. CA Cancer J. Clin. *65*, 87–108.
3. Song, Z., Wu, Y., Yang, J., Yang, D., and Fang, X. (2017). Progress in the treatment of advanced gastric cancer. Tumour Biol. *39*, 1010428317714626.
4. MacDonald, J.S., Schein, P.S., Woolley, P.V., Smythe, T., Ueno, W., Hoth, D., Smith, F., Boiron, M., Gisselbrecht, C., Brunet, R., and Lagarde, C. (1980). 5-Fluorouracil, doxorubicin, and mitomycin (FAM) combination chemotherapy for advanced gastric cancer. Ann. Intern. Med. *93*, 533–536.
5. Zhang, Y.W., Zhang, Y.L., Pan, H., Wei, F.X., Zhang, Y.C., Shao, Y., Han, W., Liu, H.P., Wang, Z.Y., and Yang, S.H. (2014). Chemotherapy for patients with gastric cancer after complete resection: a network meta-analysis. World J. Gastroenterol. *20*, 584–592.
6. Minotti, G., Menna, P., Salvatorelli, E., Cairo, G., and Gianni, L. (2004). Anthracyclines: molecular advances and pharmacologic developments in antitumor activity and cardiotoxicity. Pharmacol. Rev. *56*, 185–229.
7. Morikawa, Y., Kezuka, C., Endo, S., Ikari, A., Soda, M., Yamamura, K., Toyooka, N., El-Kabbani, O., Hara, A., and Matsunaga, T. (2015). Acquisition of doxorubicin resistance facilitates migrating and invasive potentials of gastric cancer MKN45 cells through up-regulating aldo-keto reductase 1B10. Chem. Biol. Interact. *230*, 30–39.
8. Farazi, T.A., Hoell, J.I., Morozov, P., and Tuschl, T. (2013). MicroRNAs in human cancer. Adv. Exp. Med. Biol. *774*, 1–20.
9. Galun, D., Srdic-Rajic, T., Bogdanovic, A., Loncar, Z., and Zuvela, M. (2017). Targeted therapy and personalized medicine in hepatocellular carcinoma: drug resistance, mechanisms, and treatment strategies. J. Hepatocell. Carcinoma *4*, 93–103.
10. Mihanfar, A., Fattahi, A., and Nejabati, H.R. (2017). MicroRNA-mediated drug resistance in ovarian cancer. J. Cell. Physiol. , Published online June 19, 2017. https://doi.org/10.1002/jcp.26060.
11. Wang, P., Li, Z., Liu, H., Zhou, D., Fu, A., and Zhang, E. (2016). MicroRNA-126 increases chemosensitivity in drug-resistant gastric cancer cells by targeting EZH2. Biochem. Biophys. Res. Commun. *479*, 91–96.
12. Zhang, Y., Qu, X., Li, C., Fan, Y., Che, X., Wang, X., Cai, Y., Hu, X., and Liu, Y. (2015). miR-103/107 modulates multidrug resistance in human gastric carcinoma by down-regulating Cav-1. Tumour Biol. *36*, 2277–2285.
13. Shang, Y., Zhang, Z., Liu, Z., Feng, B., Ren, G., Li, K., Zhou, L., Sun, Y., Li, M., Zhou, J., et al. (2014). miR-508-5p regulates multidrug resistance of gastric cancer by targeting ABCB1 and ZNRD1. Oncogene *33*, 3267–3276.
14. Huang, D.H., Wang, G.Y., Zhang, J.W., Li, Y., Zeng, X.C., and Jiang, N. (2015). MiR-501-5p regulates CYLD expression and promotes cell proliferation in human hepatocellular carcinoma. Jpn. J. Clin. Oncol. *45*, 738–744.
15. Jin, J., Tang, S., Xia, L., Du, R., Xie, H., Song, J., Fan, R., Bi, Q., Chen, Z., Yang, G., et al. (2013). MicroRNA-501 promotes HBV replication by targeting HBXIP. Biochem. Biophys. Res. Commun. *430*, 1228–1233.
16. Fan, D., Ren, B., Yang, X., Liu, J., and Zhang, Z. (2016). Upregulation of miR-501-5p activates the wnt/β-catenin signaling pathway and enhances stem cell-like phenotype in gastric cancer. J. Exp. Clin. Cancer Res. *35*, 177.
17. Chen, S., Zhou, Y.C., Chen, Y., Chen, X.B., Li, G.J., Lei, Y.J., Tian, L.W., Zhao, G.Q., Huang, Q., and Huang, Y.H. (2017). [Expression profile of miR-501-5p in lung adenocarcinoma patients from Xuanwei area]. Nan Fang Yi Ke Da Xue Xue Bao *37*, 354–359.
18. Sanches, J.G.P., Xu, Y., Yabasin, I.B., Li, M., Lu, Y., Xiu, X., Wang, L., Mao, L., Shen, J., Wang, B., et al. (2018). miR-501 is upregulated in cervical cancer and promotes cell proliferation, migration and invasion by targeting CYLD. Chem. Biol. Interact. *285*, 85–95.
19. Broustas, C.G., Gokhale, P.C., Rahman, A., Dritschilo, A., Ahmad, I., and Kasid, U. (2004). BRCC2, a novel BH3-like domain-containing protein, induces apoptosis in a caspase-dependent manner. J. Biol. Chem. *279*, 26780–26788.
20. Broustas, C.G., Ross, J.S., Yang, Q., Sheehan, C.E., Riggins, R., Noone, A.M., Haddad, B.R., Seillier-Moiseiwitsch, F., Kallakury, B.V., Haffty, B.G., et al. (2010). The proapoptotic molecule BLID interacts with Bcl-XL and its downregulation in breast cancer correlates with poor disease-free and overall survival. Clin. Cancer Res. *16*, 2939–2948.
21. Li, X., Kong, X., Wang, Y., and Yang, Q. (2013). BRCC2 inhibits breast cancer cell growth and metastasis in vitro and in vivo via downregulating AKT pathway. Cell Death Dis. *4*, e757.

22. Li, X., Su, P., Liu, X., Kong, X., Zhang, X., Zhang, H., and Yang, Q. (2014). Aberrant BLID expression is associated with breast cancer progression. Tumour Biol. *35*, 5449–5452.

23. Müller, I., Niethammer, D., and Bruchelt, G. (1998). Anthracycline-derived chemotherapeutics in apoptosis and free radical cytotoxicity (Review). Int. J. Mol. Med. *1*, 491–494.

24. Perego, P., Corna, E., De Cesare, M., Gatti, L., Polizzi, D., Pratesi, G., Supino, R., and Zunino, F. (2001). Role of apoptosis and apoptosis-related genes in cellular response and antitumor efficacy of anthracyclines. Curr. Med. Chem. *8*, 31–37.

25. Spangle, J.M., Roberts, T.M., and Zhao, J.J. (2017). The emerging role of PI3K/AKT-mediated epigenetic regulation in cancer. Biochim. Biophys. Acta *1868*, 123–131.

26. Xu, J., Liu, D., Niu, H., Zhu, G., Xu, Y., Ye, D., Li, J., and Zhang, Q. (2017). Resveratrol reverses Doxorubicin resistance by inhibiting epithelial-mesenchymal transition (EMT) through modulating PTEN/Akt signaling pathway in gastric cancer. J. Exp. Clin. Cancer Res. *36*, 19.

27. Garofalo, M., and Croce, C.M. (2013). MicroRNAs as therapeutic targets in chemoresistance. Drug Resist. Updat. *16*, 47–59.

28. Galluzzi, L., Senovilla, L., Vitale, I., Michels, J., Martins, I., Kepp, O., Castedo, M., and Kroemer, G. (2012). Molecular mechanisms of cisplatin resistance. Oncogene *31*, 1869–1883.

29. An, Y., Zhang, Z., Shang, Y., Jiang, X., Dong, J., Yu, P., Nie, Y., and Zhao, Q. (2015). miR-23b-3p regulates the chemoresistance of gastric cancer cells by targeting ATG12 and HMGB2. Cell Death Dis. *6*, e1766.

30. Song, B., Wang, Y., Xi, Y., Kudo, K., Bruheim, S., Botchkina, G.I., Gavin, E., Wan, Y., Formentini, A., Kornmann, M., et al. (2009). Mechanism of chemoresistance mediated by miR-140 in human osteosarcoma and colon cancer cells. Oncogene *28*, 4065–4074.

31. Song, B., Wang, Y., Titmus, M.A., Botchkina, G., Formentini, A., Kornmann, M., and Ju, J. (2010). Molecular mechanism of chemoresistance by miR-215 in osteosarcoma and colon cancer cells. Mol. Cancer *9*, 96.

32. Wang, H., Yan, C., Shi, X., Zheng, J., Deng, L., Yang, L., Yu, F., Yang, Y., and Shao, Y. (2015). MicroRNA-575 targets BLID to promote growth and invasion of non-small cell lung cancer cells. FEBS Lett. *589*, 805–811.

33. Ortega, S., Malumbres, M., and Barbacid, M. (2002). Cyclin D-dependent kinases, INK4 inhibitors and cancer. Biochim. Biophys. Acta *1602*, 73–87.

34. Milne, A.N., Sitarz, R., Carvalho, R., Polak, M.M., Ligtenberg, M., Pauwels, P., Offerhaus, G.J., and Weterman, M.A. (2007). Molecular analysis of primary gastric cancer, corresponding xenografts, and 2 novel gastric carcinoma cell lines reveals novel alterations in gastric carcinogenesis. Hum. Pathol. *38*, 903–913.

35. Sakellariou, S., Liakakos, T., Ghiconti, I., Hadjikokolis, S., Nakopoulou, L., and Pavlakis, K. (2008). Immunohistochemical expression of P15 (INK4B) and SMAD4 in advanced gastric cancer. Anticancer Res. *28* (2A), 1079–1083.

36. Matsumoto, Y., Marusawa, H., Kinoshita, K., Niwa, Y., Sakai, Y., and Chiba, T. (2010). Up-regulation of activation-induced cytidine deaminase causes genetic aberrations at the CDKN2b-CDKN2a in gastric cancer. Gastroenterology *139*, 1984–1994.

37. Li, Y., Chen, M., Liu, J., Li, L., Yang, X., Zhao, J., Wu, M., and Ye, M. (2017). Upregulation of microRNA 18b contributes to the development of colorectal cancer by inhibiting CDKN2B. Mol. Cell. Biol. *37*, e00391–e17.

38. Tamura, R.E., de Vasconcellos, J.F., Sarkar, D., Libermann, T.A., Fisher, P.B., and Zerbini, L.F. (2012). GADD45 proteins: central players in tumorigenesis. Curr. Mol. Med. *12*, 634–651.

39. Guo, W., Dong, Z., Guo, Y., Chen, Z., Kuang, G., and Yang, Z. (2013). Methylation-mediated repression of GADD45A and GADD45G expression in gastric cardia adenocarcinoma. Int. J. Cancer *133*, 2043–2053.

40. Zhang, W., Li, T., Shao, Y., Zhang, C., Wu, Q., Yang, H., Zhang, J., Guan, M., Yu, B., and Wan, J. (2010). Semi-quantitative detection of GADD45-gamma methylation levels in gastric, colorectal and pancreatic cancers using methylation-sensitive high-resolution melting analysis. J. Cancer Res. Clin. Oncol. *136*, 1267–1273.

41. Lu, Y.J., Wu, C.S., Li, H.P., Liu, H.P., Lu, C.Y., Leu, Y.W., Wang, C.S., Chen, L.C., Lin, K.H., and Chang, Y.S. (2010). Aberrant methylation impairs low density lipoprotein receptor-related protein 1B tumor suppressor function in gastric cancer. Genes Chromosomes Cancer *49*, 412–424.

42. Wu, C.S., Lu, Y.J., Li, H.P., Hsueh, C., Lu, C.Y., Leu, Y.W., Liu, H.P., Lin, K.H., Hui-Ming Huang, T., and Chang, Y.S. (2010). Glutamate receptor, ionotropic, kainate 2 silencing by DNA hypermethylation possesses tumor suppressor function in gastric cancer. Int. J. Cancer *126*, 2542–2552.

43. Kim, J., Min, S.Y., Lee, H.E., and Kim, W.H. (2012). Aberrant DNA methylation and tumor suppressive activity of the EBF3 gene in gastric carcinoma. Int. J. Cancer *130*, 817–826.

44. Cui, Y., Ying, Y., van Hasselt, A., Ng, K.M., Yu, J., Zhang, Q., Jin, J., Liu, D., Rhim, J.S., Rha, S.Y., et al. (2008). OPCML is a broad tumor suppressor for multiple carcinomas and lymphomas with frequently epigenetic inactivation. PLoS ONE *3*, e2990.

OMTN, Volume *12*

Supplemental Information

A Novel Mechanism of Doxorubicin Resistance and Tumorigenesis Mediated by MicroRNA-501-5p-Suppressed BLID

Yun-chao Xu, Xu Liu, Min Li, Yan Li, Chun-yan Li, Ying Lu, Jaceline Sanches, Lu Wang, Yue Du, Li-min Mao, Si-bo Zuo, Hui-ting Liu, Jie Shen, Bo Wang, Li Hou, Lian-hong Li, Jian-wu Tang, Jing-fang Ju, Hong-wei Guan, and Bo Song

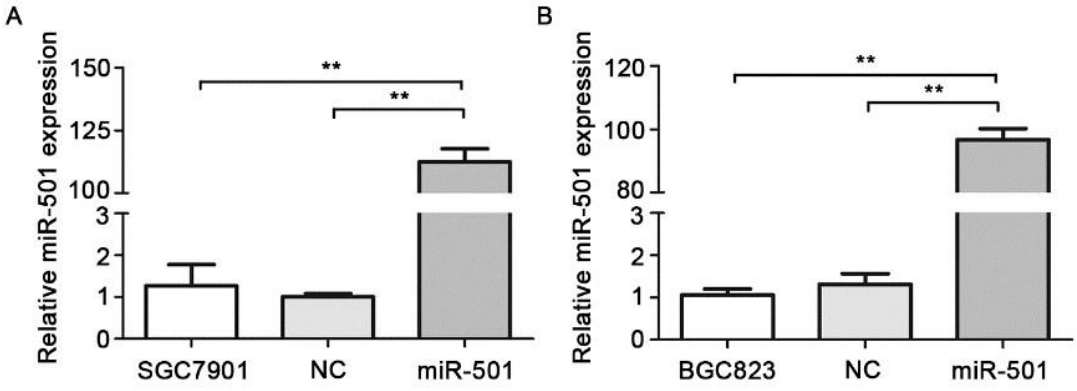

Figure S1 miR-501 is overexpressed in SGC7901 and BGC823 cells after transfected with miR-501 mimic. The level of miR-501 was detected by real-time qRT-PCR analysis. The negative miRNA (NC) and SGC7901 and BGC823 cells were the negative controls, respectively. The experiments were repeated for three times and the numbers are indicated as mean ± SD. $^{**}P < 0.01$.

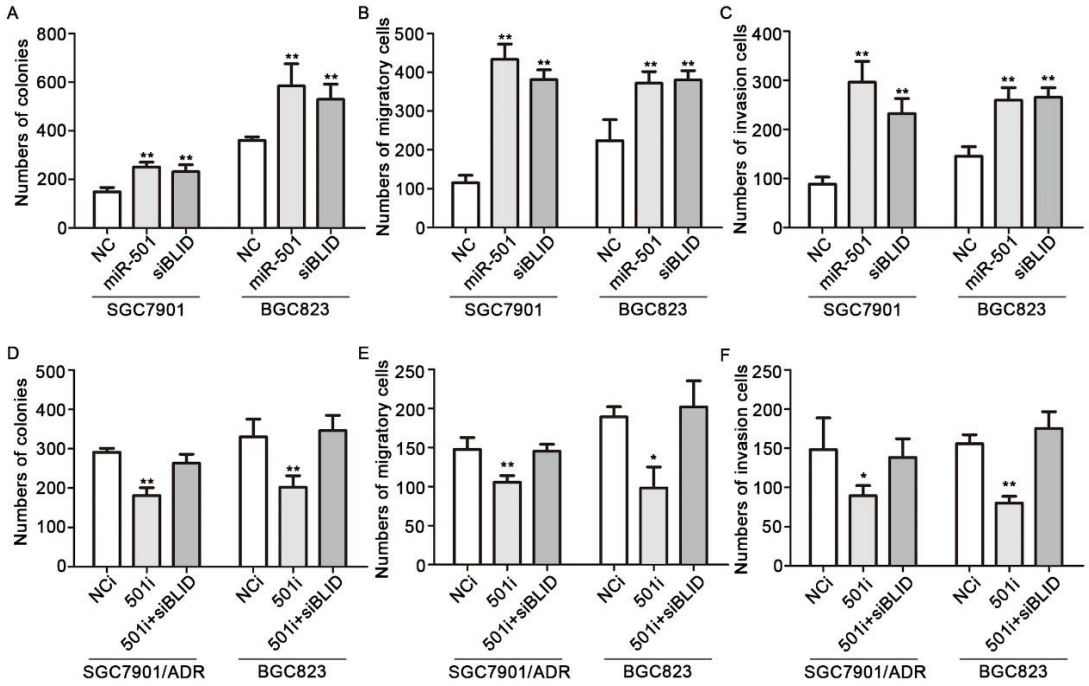

Figure S2 Graph data and statistical analysis of cell proliferation, migration and invasion. (A) SGC7901 and BGC823 cells were transfected with the miRNA mimics or siRNA described as above. The colony formation assay was performed to show the impact of miR-501 on cell growth. **(B)** Cell migratory potential was determined by the transwell migration assay without matrigel. **(C)** Cell invasive potential was determined by the transwell invasion assay with matrigel. **(D)** The endogenous miR-501 was knocked down by the inhibitor in SGC7901/ADR and BGC823 cells. The cell proliferative potential was detected by colony formation assay. Transwell assays with or without matrigel were performed to determine the potentials of migration **(E)** and invasion **(F)** in the miR-501 knockdown SGC7901 cells and BGC823 cells, respectively. All the experiments were repeated for three times and the numbers are indicated as mean ± SD. **P* < 0.05, ***P* < 0.01.

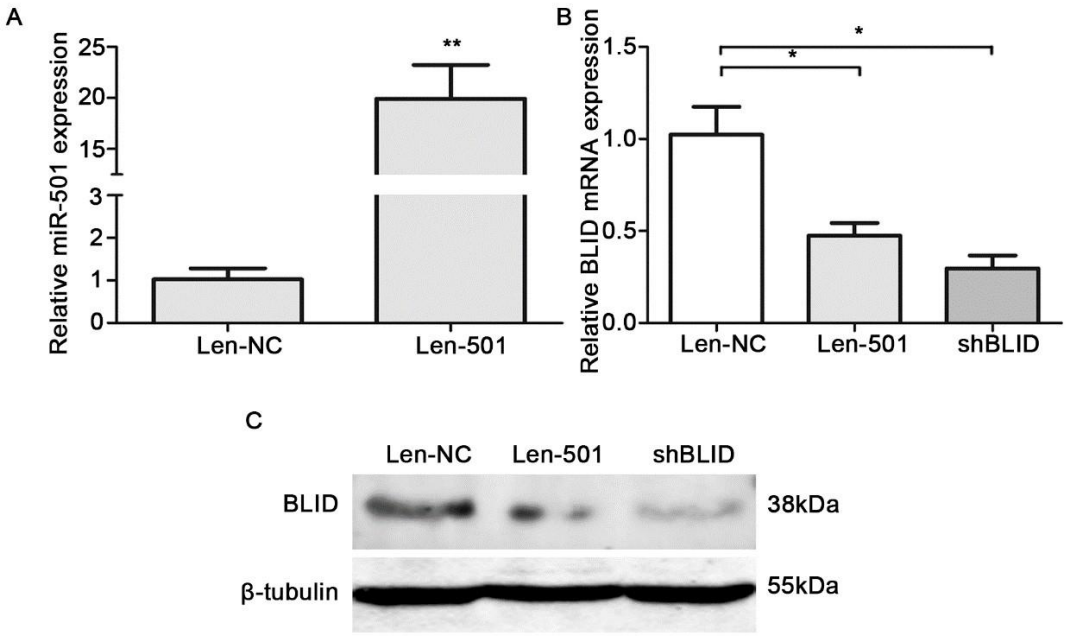

Figure S3 miR-501 is upregulated and BLID is downregulated in the miR-501 lentivirus infected SGC7901 cells. (A) SGC7901 cells were infected with lentiviral vectors of miR-501 (Len-501), negative control (Len-NC), or shRNA against BLID (shBLID). The expression of miR-501 was quantified by real-time qRT-PCR. **(B)** The expression of BLID mRNA was detected by real-time qRT-PCR. (C) The expression of BLID protein was analyzed by Western blot. The experiments were repeated for three times and the numbers are indicated as mean ± SD. *$P < 0.05$, **$P < 0.01$.

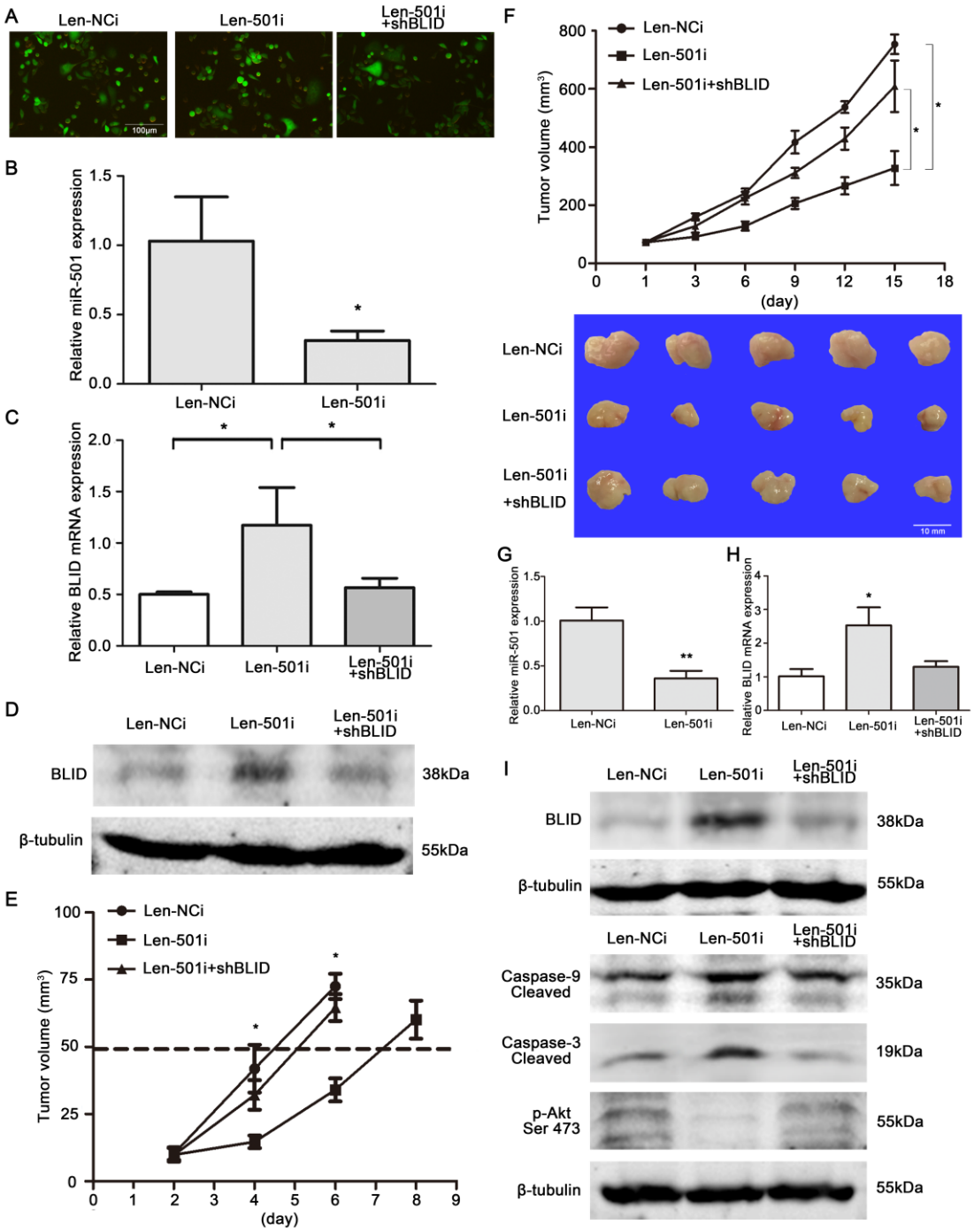

Figure S4 miR-501 knock-down reverses doxorubicin resistance and inhibits the growth of gastric cancer cell *in vivo*. (A) SGC7901 cells were infected with lentiviral vectors of miR-501 inhibitor (Len-501i), scrambled miRNA inhibitor (Len-NCi) or were co-infected with lentiviral vectors of miR-501 inhibitor and shRNA against BLID (Len-501i + shBLID). The cells with green fluorescence were observed under the fluorescence microscope and the representative pictures were shown. **(B)**

miR-501 expression was measured by real-time qRT-PCR in Len-NCi and Len-501i groups of cells. **(C)** BLID mRNA expression was detected by real-time qRT-PCR. **(D)** BLID protein expression was analyzed by Western blot. **(E)** The growing rate curve of the subcutaneous tumors in nude mice was shown. **(F)** The tumor volumes were measured and recorded at all the time points during ADR treatment. **(G)** The expression of miR-501 in tumor xenografts was quantified by real-time qRT-PCR. **(H)** The expression of BLID mRNA in the mice xenograft tumor tissues was detected using real-time qRT-PCR. **(I)** The protein expression of BLID, cleaved caspase-9/3 and p-Akt Ser 473 in the xenograft tumor tissues were analyzed by Western blot. Numbers are indicated as mean ± SD. *$P < 0.05$, **$P < 0.01$.

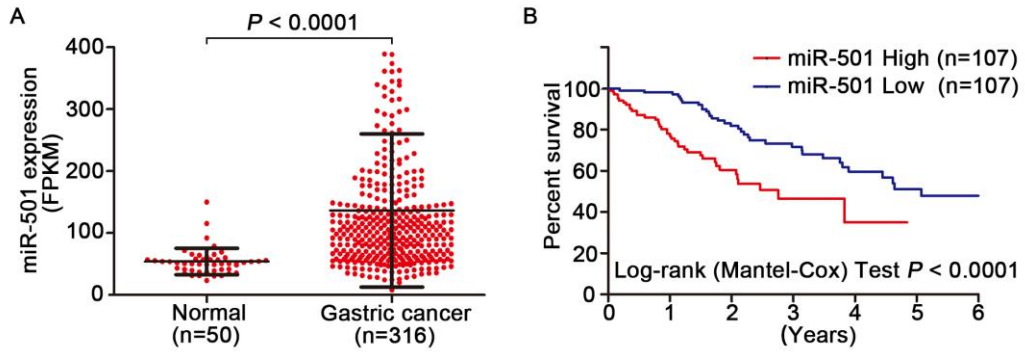

Figure S5 miR-501 is upregulated in the gastric cancer tissues and predicts the poor prognosis based on The Cancer Genome Atlas (TCGA) dataset analysis. (A) Comparison of miR-501 level in normal gastric tissues (n = 50) with gastric cancer tissues (n = 316). **(B)** Kaplan-Meier plots were used to estimate overall survival rate. Log rank test was performed to assess the differences in survival between the high (n = 107) and low of miR-501 expression group (n = 107). The experiments were repeated for three times and the numbers are indicated as mean ± SD.

Table S1 Primer sequences or lot numbers of real-time qRT-PCR

Name	Primer sequences or Lot numbers
BLID	Forward 5’ - CCTCTGCTGAGGCCCTGTAA - 3’
	Reverse 5’ - GCCTGAATAATGGGCGAAATC - 3’
GAPDH	Forward 5’ - CCACTCCTCCACCTTTGAC - 3’
	Reverse 5’ - ACCCTGTTGCTGTAGCCA - 3’
miR-501	Applied Biosystems Lot Number: P161011-002 H09 (Thermo Fisher Scientific, Waltham, MA)
RNU6B	Applied Biosystems Lot Number: P160808-004 E06 (Thermo Fisher Scientific, Waltham, MA)

Table S2 Sequences of synthesized oligonucleotides for miR-501 binding site(s) of BLID

3'UTR	Location	Sequences of oligonucleotides
BLID mRNA	87-242bp	Forward - wild type: 5'TCTAGATTCAATAAGACCCAATTCTTAACAGTCTT TTCTACCCACTTTTACCCATAACTTTTCCAAATTTG GTTCAAATTGTGCAGAGAAACAATAAAATTTTTAA AAAGGATAAACTGGCTAGTTAAAAGTAAATGGCAT TTAATTAAAACAAATCTTGCATCTAGA 3' Reverse - wild type: 5'TCTAGATGCAAGATTTGTTTTAATTAAATGCCATT TACTTTTAACTAGCCAGTTTATCCTTTTTAAAAATTT TATTGTTTCTCTGCATAATTTGAACCAAATTTGGAA AAGTTATGGGTAAAAGTGGGTAGAAAAGACTGTTA AGAATTGGTCTTATTGAATCTAGA 3' Forward - mutant: 5'TCTAGATTCAATAAGACCCAATTCTTAACAGTCTT TTCTACCCACTTTTACCCATAACTTTTCCAAATTTG GTTCAAATTGTGCAGAGAAACAATAAAATTTTTAA *CCCTTCG*AAACTGGCTAGTTAAAAGTAAATGGCAT TTAATTAAAACAAATCTTGCATCTAGA3' Reverse - mutant: 5'TCTAGATGCAAGATTTGTTTTAATTAAATGCCATT TACTTTTAACTAGCCAGTTTCGAAGGGTTAAAAAT TTTATTGTTTCTCTGCATAATTTGAACCAAATTTGG AAAAGTTATGGGTAAAAGTGGGTAGAAAAGACTG TTAAGAATTGGTCTTATTGAATCTAGA3'

Underlined bases are the predicted binding sites; italic base pairs are mutant.